An algorithm for the calculation of the light distribution in photovoltaic greenhouses

Article *in* Solar Energy · January 2017

DOI: 10.1016/j.solener.2016.11.024

8 authors, including:

Marco Cossu
Università degli Studi di Sassari

Luigi Ledda
Università Politecnica delle Marche

Antonella Sirigu
Agris Sardegna, Cagliari, Italy

Andrea Cossu
Middlesex University, UK

Solar Energy 141 (2017) 38–48

Contents lists available at ScienceDirect

Solar Energy

journal homepage: www.elsevier.com/locate/solener

An algorithm for the calculation of the light distribution in photovoltaic greenhouses

Marco Cossu [a,*], Luigi Ledda [b], Giulia Urracci [c], Antonella Sirigu [c], Andrea Cossu [d], Lelia Murgia [e], Antonio Pazzona [e], Akira Yano [a]

[a] Faculty of Life and Environmental Science, Shimane University, 1060 Nishikawatsu, Matsue, Shimane 690-8504, Japan
[b] Department of Agriculture, Division of Agronomy and Plant Genetics, University of Sassari, Viale Italia 39, 07100 Sassari, Sardinia, Italy
[c] Agris Sardegna, Department of Plant Science, Viale Trieste 111, 09123 Cagliari, Sardinia, Italy
[d] Food Science and Technology Department, University of California – Davis, Davis, CA 95616, USA
[e] Department of Agriculture, Division of Agricultural Engineering, University of Sassari, Viale Italia 39, 07100 Sassari, Sardinia, Italy

ARTICLE INFO

Article history:
Received 28 March 2016
Received in revised form 2 November 2016
Accepted 11 November 2016

Keywords:
Renewable energy
Solar radiation
Crop
Shading

ABSTRACT

This study introduces a novel algorithm to estimate the cumulated global radiation inside photovoltaic (PV) greenhouses at the desired time interval. The direct and diffuse radiation were calculated on several observations points (OPs) inside the PV greenhouse. The PV panels were assimilated to polygons that can overlap the sun path seen from a specific OP. The algorithm was tested in a greenhouse with 50% PV cover ratio on the roof. The results were showed as the percentage ratio of the cumulated yearly global radiation with and without PV array on the roof (G_{GR}), and used to draw maps of light distribution on different canopy heights (from 0.0 to 2.0 m). The maps displayed the variability of the light distribution and the most adversely affected zones inside the PV greenhouse. The yearly G_{GR} increased with the canopy height on the zones under the plastic cover (G_{GR} from 59% at 0.0 m to 73% at 2.0 m), and decreased under the PV cover (G_{GR} from 57% at 0.0 m to 40% at 2.0 m). Most zones close to the side walls and the gable walls were the least affected by shading on all canopy heights. The different light distribution on the canopy heights showed that the incident solar energy on the crop changes consistently, according to the growth stage of the plants. The algorithm can be applied to several PV greenhouse types and may provide a decision support tool for the identification of the most suitable plant species, based on their light requirements.

1. Introduction

Renewable energy sources have increased the productivity and competitiveness of the agricultural sector, contributing positively to its environmental sustainability. The photovoltaic (PV) energy has been the most successful renewable source applied in European agriculture, primarily due to the long life, reliability and broad application of the technology. These features have been considered in the design of new crop systems, defined "agrivoltaic" systems, which integrate energy and food production on the same land unit (Dupraz et al., 2011). The PV greenhouse achieves this goal by integrating the PV panels on the roof. This is useful especially in locations where the land resource is limited (Dinesh and Pearce, 2016). Under this point of view, PV greenhouses can be considered an example of Building Integrated Photovoltaic (BIPV) systems, because the shading is useful for both the power generation and for reducing the cooling load of the building (Yoo, 2011). The installations often occupy large areas of land, since they are specifically built for PV energy massive production, resulting in an ecological impact on the agricultural ecosystems. The application of the solar architecture principles allows the installation of PV modules in more environmental friendly ways, improving the indoor environmental quality of the building (Yoo, 2015).

The PV greenhouses are particularly efficient in high solar irradiation regions, such as southern Europe (Campiotti et al., 2008). These structures consist of large-scale investments designed to maximize the energy production by avoiding any shading on the PV array (from objects or nearby greenhouses), choosing an East (E) – West (W) orientation, corresponding to South (S) – oriented PV roofs, and providing the greenhouse with openings designed to cool down the back cover of the PV modules, aiming to an optimised efficiency. The inverters are usually placed inside the PV greenhouse, exploiting the cooling effect of the shading cast by the PV array, thus optimizing the energy conversion efficiency.

* Corresponding author.
E-mail addresses: marcocossu@uniss.it, marcocossu@life.shimane-u.ac.jp (M. Cossu).

http://dx.doi.org/10.1016/j.solener.2016.11.024

Nomenclature

c	correction coefficient for summer time (h)
CV	coefficient of variation (%)
E	equation of time (rad)
G_{GR}	cumulated global radiation on the PV greenhouse area (%)
I_0	solar constant (1367 W m^{-2})
I_d	diffuse radiation (W m^{-2})
I_D	direct radiation (W m^{-2})
I_G	greenhouse global radiation on horizontal plane (W m^{-2})
I_{GP}	global radiation on the OP (W m^{-2})
LAT	local apparent time (h)
LMT	local time, or "clock time" (h)
m	number of OPs considered (–)
n	number of the day of the year
p	atmospheric transmissivity coefficient (–)
R^2	coefficient of determination (%)
x_e, y_e, z_e	cartesian coordinates of an edge of the PV panel (m)
x_{op}, y_{op}, z_{op}	cartesian coordinates of the OP (m)
β	angle of the equation of time (rad)
δ	the solar declination angle (rad)
θ	solar elevation angle (rad)
θ_e	elevation angle of the OP (rad)
λ	longitude of the location (°)
λ_R	longitude of the time zone of the location (°)
τ	overall greenhouse transmissivity (–)
Ψ	azimuth angle of the sun (rad)
Ψ_e	azimuth angle of the OP (rad)
ω	hour angle (rad)
ϕ	latitude of the location (rad)

The maximization of the energy production is considered crucial to ensure the high profitability of the investment, which relies only on the favorable public subsidies supplied for the PV energy generation. In fact, the high economic incentives provided by some European countries for PV energy generation in the last 7 years triggered the construction of new large PV greenhouse installations, which agronomic performance is in most cases negatively affected by the low level of solar radiation (Cossu et al., 2014; Fatnassi et al., 2015).

These issues address current researches to the agronomic sustainability of the PV greenhouse systems, focusing in particular on the design optimisation, the development of new PV technologies and the selection of plant species suitable for the solar light limitations inside PV greenhouses (Poncet et al., 2012). The greenhouses catch about two thirds of the available solar radiation and their efficiency is strongly related to their position and geometry, which are determined by horticultural constraints (Pieters and Deltour, 1999). This efficiency further decreases due to the PV panels on the roof. As a consequence, the characterisation of the internal environmental conditions is essential to evaluate the agronomic sustainability of the PV greenhouses. In particular, the analysis should be conducted primarily on the available solar light and its distribution on the greenhouse area. The measurements of the daily solar radiation with weather stations are scarce and dispersed for operational use in crop growth simulation models (Supit and Van Kappel, 1998). For this reason, specific models are required to provide effective solar radiation data for agronomic purposes.

Various studies have been conducted to provide decisional support for new design criteria and management of PV greenhouses. Some authors applied numerical simulations, including the Computational Fluid Dynamic (CFD) to assess the PV greenhouse microclimate in terms of solar radiation, temperature and air flow for specific summer and winter days (Fatnassi et al., 2015; Serrano-Arellano et al., 2015). The evolution of temperature and humidity inside PV greenhouses have been simulated also using the TRNSYS (Transient System Simulation Tool) software, highlighting that the winter night temperature inside a PV greenhouse under a sudden fall until ambient temperature, while the summer temperature was too high for greenhouse crops (Carlini et al., 2010, 2012). TRNSYS has been applied also to evaluate the solar water heating systems for greenhouse microclimate control, to calculate the productivity of the PV array, and to analyse the environmental parameters inside a prototype greenhouse equipped with semi-transparent PV panels and vertical farm systems for urban agriculture (Attar and Farhat, 2015; Bambara and Athienitis, 2015). Geostatistics approaches have been used to assess the variability of the thermal spatial distribution, suggesting that the results of the crop growth models cannot be generalized for the entire greenhouse area due to the variability of the microclimate patterns (Bojacá et al., 2009). Yano et al. proposed an equation-based procedure to calculate the solar radiation impinging on a specific point located inside a PV greenhouse with 12.9% cover ratio, comparing the straight-line and a checkerboard installation pattern of the PV panels the roof (Yano et al., 2009, 2010). Castellano calculated the solar radiation distribution inside a greenhouse with different PV installation patterns and roof cover ratio on specific days, by using the software Autodesk® Ecotect® Analysis (Castellano, 2014; Castellano et al., 2016). The variability of the shade distribution was calculated as percentage of shading, which changed accordingly to the sun position, the configurations of the PV panels on the roof and the zones considered inside the greenhouse.

The software packages and the methods proposed in literature calculate the direct and diffuse light inside the PV greenhouse only on a specific date and time, while the agronomic performance of the PV greenhouse should consider the cumulated light distribution on the crop cycle basis for a reliable crop yield estimation. The cumulated values of solar radiation inside the greenhouse can be simulated by calculating the external solar radiation on the horizontal and inclined plane. This can be obtained by determining the astronomical parameters related to the solar geometry in terms of sun elevation and sun azimuth, as a function of the geographic coordinates of the study location (El Mghouchi et al., 2016; Gueymard, 2000; Markvart, 2000; Shen et al., 2008). The direct and diffuse radiation can be simulated using equations based on the astronomical parameters and the atmospheric conditions. Some of them are empirical and use dimensionless coefficients for estimating the effect of the atmosphere, such as the Ghouard model or the Perrin de Brichambaut model (El Mghouchi et al., 2016; Perrin de Brichambaut, 1975; Saïghi, 2002). The Collares-Pereira and Rabl model uses semi-empirical expressions, coupling equations and coefficients, showing to be very accurate, especially for predicting the monthly mean hourly global radiation (Collares-Pereira and Rabl, 1979; Wan Nik et al., 2012). In addition, more complicated models, such as the Capderou model and the Bird and Hulstrom model, include the turbidity factor to calculate the direct and diffuse solar radiation components (Bird and Hulstrom, 1980; Capderou, 1985). In particular, they implement the absorption and diffusion factor of the atmospheric gases, such as ozone, gas, water and other aerosols. Lastly, other simplified models include few variables, allowing a faster calculation, and are suitable for estimating the greenhouse global radiation on the top of canopies, such as the Bouguer and Berlage equations applied in the present paper, which considers the general atmospheric transmissivity without the absorbed and reflected solar flux by the atmospheric components (Berlage, 1928; Kosugi et al., 2006).

In PV systems energy estimation, the reduction in energy yield due to the shadow cast by obstacles surrounding the PV array can be estimated following two possible approaches. The first is to simulate the shadow cast on the PV array and their variation in time by using an heliodon, and calculate the direct and diffuse irradiance (Blewett et al., 1997; Woyte et al., 2003). The second approach is the estimation of the reduced irradiation as seen from an observer point on the PV array, considered as polygons expressed in cylindrical coordinates by means of optical instruments (Quaschning and Hanitsch, 1998). We decided to follow this latter concept, given its flexibility for application in different contexts. However, the procedure had to be modified for a new scope, since the irradiance must be calculated on the greenhouse area and each PV module becomes a small obstacle to the solar radiation input on the crop. According to this, we introduced an algorithm which can calculate the cumulated distribution of the solar radiation inside a PV greenhouse at the desired time interval, as a function of the shading cast by the PV array on the roof. The procedure is based on a geometric condition assimilating the PV panels to polygons that can overlap the sun path observed from specific observation points located inside the greenhouse. The calculation can be reiterated for multiple points and used to draw maps of cumulated light distribution on yearly basis and on different canopy heights. The validation was conducted on a real PV greenhouse with 50% cover ratio. This algorithm can be applied to various PV greenhouse types with different location, orientation, roof slope, PV cover ratio and installation patterns of the PV panels on the roof.

2. Materials and methods

2.1. Characteristics of the photovoltaic greenhouse

The algorithm was applied and validated on a commercial pitched-roof PV greenhouse in Decimomannu (Sardinia, Italy; 39°19′59″N, 8°59′19″E), already used by the authors for previous experiments concerning the measurement of the light distribution inside PV greenhouses (Cossu et al., 2014). The area of the greenhouse was 960 m^2 and it was provided with two spans (50.0 m long and 9.6 m wide each), gutter height of 2.5 m, roof slope of 22° and E–W orientation (Fig. 1). The plastic cover and the walls were made with polyvinyl chloride (PVC, Ondex Bio, Renolit, France), with a nominal light transmissivity up to 90% declared by the manufacturer (transparency to short infrared 90%; to ultraviolet 8%; to long infrared 99%). The cladding material and the PV panels were supported by a steel structure. The S oriented roof of each span was formed by 144 multi-crystalline silicon PV modules (REC 235PE, REC Solar, USA), with dimensions 1665 × 99 × 138 mm. As a result, 50% of the roof area was covered with PV modules. The total PV area was 475 m^2 (238 m^2 per span), while the total active cell area was 420 m^2. The peak rated power of the PV system was 68 kWp.

The cumulated yearly light distribution was calculated on different canopy heights (0.0, 0.5, 1.0, 1.5 and 2.0 m from the ground level). Calculations were conducted on 5 sets of observation points (OPs), each one formed by 27 OPs. Set G1 and G2 were located 1.5 m from the gable walls of the greenhouse. Set S1, S2 and S3 were placed equidistant. This distribution was chosen according to previous observations inside the same PV greenhouse, stating that the variability of the light distribution on the E-W direction is not statistically significant inside E-W oriented PV greenhouses (Cossu et al., 2014). For this reason, a lower amount of OPs is enough to quantify the distribution on the E-W direction (5 OPs), compared to the number of OPs on the N-S direction (27 OPs). In addition, the solar radiation incident on the zones close to the gable walls is different from what observed on the remaining area (Castellano, 2014). As a consequence, the evaluation of the incident light close to the gable walls is necessary to accurately describe the distribution on the whole PV greenhouse.

2.2. Algorithm for the calculation of the light distribution inside the photovoltaic greenhouse

2.2.1. Calculation of the incident global radiation

The position of the sun was determined using the solar elevation angle and the solar azimuth angle in radians for the whole year, at 1 h interval (Fig. 2). θ has positive values above the horizon

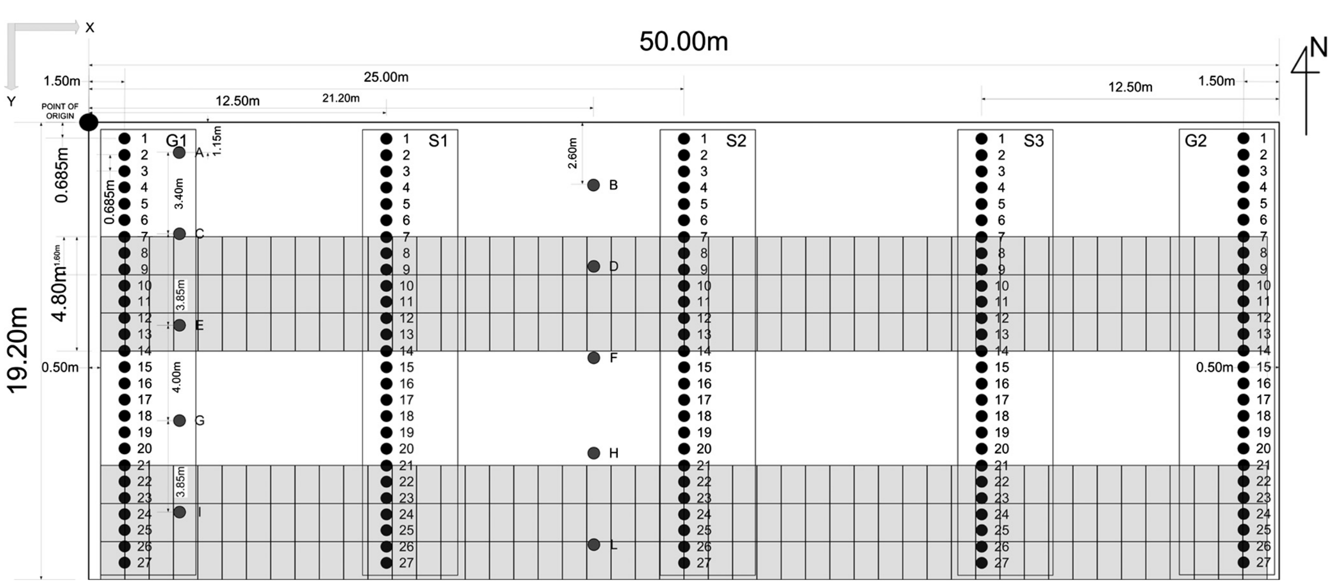

Fig. 1. Map of the PV greenhouse and position of the sets of OPs for the calculations. The OPs in grey and alphabet letters indicate the position of the pyranometers used for validating the model. The x and y axis for the Cartesian coordinates of the PV panels and the OPs are also displayed.

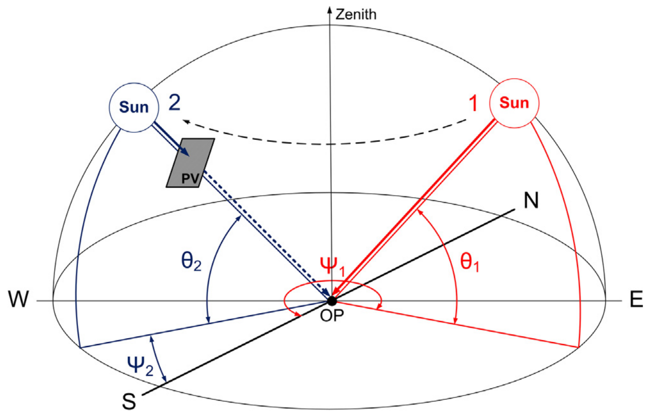

Fig. 2. Solar elevation angle and azimuth angle of the sun, in relation to the position of the PV panel and the observation point OP. The case 1 depicts a position of the sun in which the OP is under direct sunlight; in case 2 the OP is under the shading of the PV panel. θ and Ψ are the solar elevation and the solar azimuth angles, respectively.

(0 rad on the horizon plane) and it was calculated according to the following equation (Markvart, 2000; Page, 2003; Yano et al., 2009):

$$\theta = \text{Arcsin}(\text{Sin}\phi\ \text{Sin}\delta + \text{Cos}\phi\ \text{Cos}\delta\ \text{Cos}\omega) \tag{1}$$

where (Markvart, 2000; Page, 2003):

$$\omega = \frac{\pi}{12}(LAT - 12) \tag{2}$$

$$\delta = \pi\frac{23.45}{180}\text{Sin}\left(2\pi\frac{284+n}{365}\right) \tag{3}$$

LAT was calculated using the formula (Page, 2003):

$$LAT = LMT + \frac{(\lambda - \lambda_R)}{15} + E - c \tag{4}$$

E is expressed with (Markvart, 2000):

$$E = 2.292(0.0075 + 0.1868\text{Cos}\beta - 3.2077\text{Sin}\beta - 1.4615\text{Cos}2\beta - 4.089\text{Sin}2\beta) \tag{5}$$

where β is an angle expressed in radians and equal to:

$$\beta = \frac{2\pi(n-1)}{365} \tag{6}$$

Ψ is (Markvart, 2000; Page, 2003):

$$\Psi = \text{Arccos}\left(\frac{\sin\theta\sin\phi - \sin\delta}{\cos\theta\cos\phi}\right) \tag{7}$$

The angle is 0 to the S direction and it was multiplied by -1 when $\sin\Psi < 0$.

2.2.2. Calculation of the internal global radiation

The direct and diffuse radiation on the horizontal plane were calculated according to the following Bouguer and Berlage equations, assuming clear sky conditions (Berlage, 1928; Reiter et al., 1982; Palva et al., 2001; Tanaka et al., 2002; Kosugi et al., 2006):

$$I_D = I_0 \cdot p^{\frac{1}{\text{Sin}\theta}} \cdot \text{Sin}\theta \tag{8}$$

The diffuse radiation is:

$$I_d = \frac{I_0\text{Sin}\theta\left(1 - p^{\frac{1}{\text{Sin}\theta}}\right)}{2(1 - 1.4\text{Log}\,p)} \tag{9}$$

I_G was considered as the sum of the direct and diffuse radiation:

$$I_G = \tau(I_D + I_d) \tag{10}$$

where the overall light transmissivity of the greenhouse τ is due to the frame and the cover material. I_G can be considered as the incident global radiation inside the greenhouse without any PV panels installed on the roof. Therefore, this parameter was considered to calculate the percentage availability of global radiation inside the PV greenhouse as a function of the global radiation inside a conventional greenhouse.

2.2.3. Determination of the global radiation on a random OP inside the PV greenhouse

The functions used in the present algorithm were implemented in the software Wolfram Mathematica (Wolfram, 2014). To determine the actual solar radiation on the OPs, each PV panel on the greenhouse roof was considered as a polygon with 4 edges by using the geometric function "Polygon" of the software. The Cartesian coordinates (x, y, z) of the 4 edges and the OP were calculated as a function of an arbitrary point of origin located in the North (N)-E edge of the greenhouse. The Cartesian coordinates of the PV panels were then converted into solar coordinates, thus θ_e and Ψ_e, in relation to a specific OP (which can also represent the position of a single plant on the greenhouse area), by using the following expressions:

$$\theta_e = \text{Arcsin}\frac{z_e - z_{op}}{\sqrt{(x_e - x_{op})^2 + (y_e - y_{op})^2 + (z_e - z_{op})^2}} \tag{11}$$

$$\Psi_e = \text{Arccos}\frac{y_e - y_{op}}{\sqrt{(x_e - x_{op})^2 + (y_e - y_{op})^2}} \tag{12}$$

Ψ_e is equal to 0 on S and it was considered negative when $x_e - x_{op} < 0$, thus when it moved towards W.

The solar coordinates of the 4 edges of the PV panel ($\theta_e^{1,2,3,4}$, $\Psi_e^{1,2,3,4}$) were compared to the solar coordinates of the sun (θ, Ψ) seen from the OP, by using the function "Region Member" of the software, to verify when the solar coordinates cast on the PV panel surface area (Fig. 3). When the solar coordinates of the sun were inside the area of the polygon, the OP was considered under the shadow of the PV panel, thus without incident direct radiation. As a consequence, the global radiation on the OP (I_{GP}) was equal to the diffuse radiation ($I_{GP} = I_d$). On the contrary, when the sun coordinates were outside the area of the PV panel, the OP was considered under sunlight, thus receiving both direct and diffuse radiation ($I_{GP} = I_D + I_d$). This procedure was applied simultaneously for all the panels of the PV system on a single OP and then reiterated for all OPs.

The incident global radiation on the PV greenhouse area (G_{GR}) was calculated as the mean percentage ratio of I_{GP} of all m OPs and I_G, which can be considered as the potential global radiation inside the same greenhouse without PV array on the roof:

$$G_{GR} = \frac{1}{m}\sum_{OP=1}^{m}\frac{I_{GP}}{I_G} \cdot 100 \tag{13}$$

where m was varied to calculate the G_{GR} for specific zones of the PV greenhouse. It is well known that the transmissivity of the cladding material is related to the sun beam incidence angle, the condensation, the dust accumulation and ageing (Al-Mahdouri et al., 2014; Kitta et al.,, 2014; Pollet and Pieters, 2002). In particular, the maximum nominal transmissivity is measured with an incidence angle of the sun beam normal to the cover and decreases with the increase of the angle of incidence. The angle of incidence on the

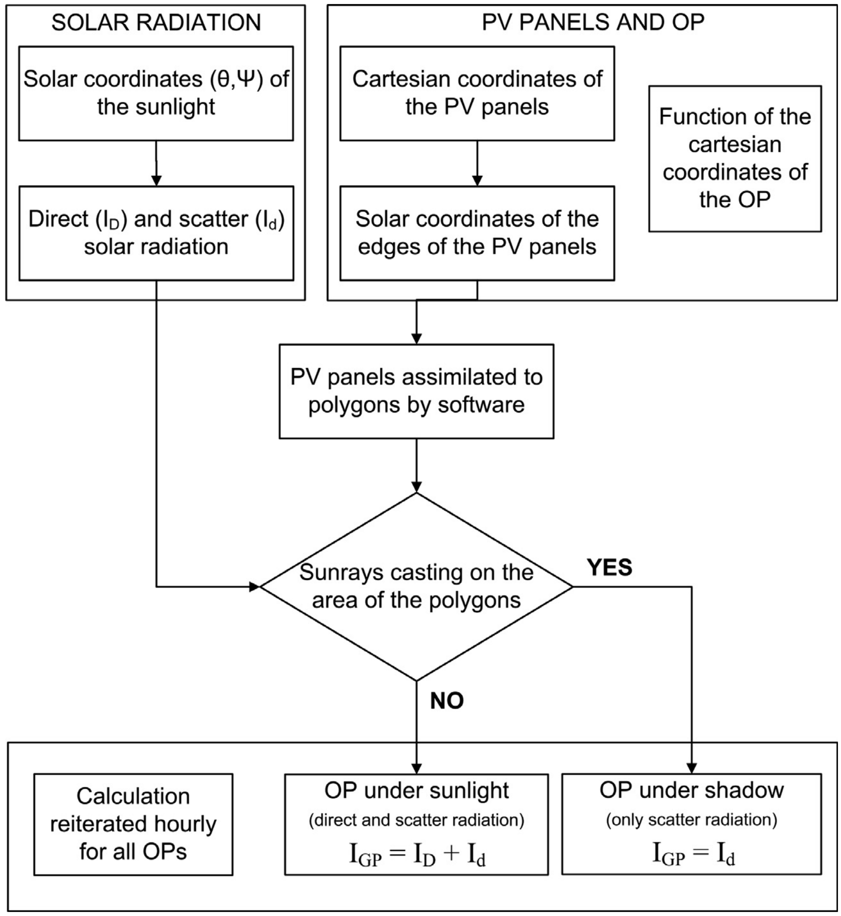

Fig. 3. Flow chart of the calculation and decisional process operated by the model via software.

greenhouse roof is minimum in the central part of the day, and higher in the morning and evening.

To avoid the variability due to the transmissivity of the cladding material, the PV greenhouse global radiation was expressed using a ratio: in fact, both the numerator (I_{GP}) and denominator (I_G) of the ratio were calculated multiplying the calculated value for τ, thus leading to a G_{GR} independent from the cladding transmissivity. As a consequence, G_{GR} describes the light distribution only as a function of the PV greenhouse type (dimensional parameters and PV cover ratio), assuming a general validity also when the same PV greenhouse is assembled in different locations or using different cladding materials.

2.2.4. Validation of the model

The model was validated by measuring the global radiation inside the real PV greenhouse on 12 days with clear sky (one per month), from May 2013 to April 2014. The measurements were conducted using 10 pyranometers (HOBO Silicon Pyranometer Sensor w/3 m Cable - cod. S-LIB-M003; Onset Computer Corporation, Bourne, USA), placed at 1.3 m height and indicated using letters (from A to L), according to the pattern depicted in Fig. 1. All data were collected with a single datalogger (HOBO Micro Station Logger G21-002; Onset Computer Corporation, Bourne, USA) at 1 min interval and averaged every 15 min. The external global radiation data were collected from the closest weather station located in Uta (Sardinia, Italy; 39°17′35.1″N 8°55′55.0″E). The sky transmissivity coefficient on the single day was estimated adjusting the calculated external global radiation to best correlate with the corresponding external measured values. The mean greenhouse transmissivity was calculated on each sensor position from 7:00 to 18:00 h, as the ratio of the global radiation measured by the sensor and the external global radiation. To mitigate the effect of the shadow cast by the metallic frame on the roof (not considered by the present algorithm), the measurements of the sensors were corrected using the mean hourly greenhouse transmissivity: when the measured transmissivity on the sensor was lower than the daily mean greenhouse transmissivity, the values were adjusted by multiplying the daily mean transmissivity for the external global radiation.

The variability of the light distribution was studied using the Coefficient of Variation (CV), thus the ratio of the standard deviation and the mean global radiation on the OPs. The validation was conducted using the Coefficient of Determination (R^2) between measured and calculated data, the Mean Bias Error (MBE), the Relative Mean Square Error (RMSE), which are supposed to be used in conjunction and that can be considered the main and most popular statistical parameters to assess the performance of solar radiation models (El Mghouchi et al., 2016; Stone, 1993; Supit and Van Kappel, 1998; Wan Nik et al., 2012). In addition, the Relative Root Mean Square Error (RRMSE) was calculated by dividing the RMSE for the mean daily global radiation measured by the pyranometers.

3. Results and discussion

3.1. Solar light distribution in the photovoltaic greenhouse

The calculated data were compared to the 12 days of measurements used for the validation on each pyranometer, showing a mean R^2 of 0.88 ± 0.06 (Table 1). The MBE was usually positive, indicating a slight overestimation of the calculated values, compared to the ones measured by the pyranometers. The absolute values of both MBE and RMSE were low on point H and also on point D and L (under the PV cover). The highest values of MBE and RSME were calculated on point A (0.121 and 0.534 MJ m^2 d^{-1}, respectively). The accuracy of a model is considered excellent when RRMSE is from 0% to 10%, good if it is between 10% and 20%, fair from 20% to 30% and poor over 30% (Li et al., 2013; Despotovic et al., 2015). According to this, the present model performed well for all the measured points, with a maximum RRMSE of about 17%.

Depending on how the solar coordinates intersect the PV array coordinates, the OPs can be under three basic conditions: direct light, partial shading or complete shading (Fig. 4). In summer the solar elevation angle on OP F was high and the sun path moved above the PV array, leaving the OP under direct radiation for all day (June 16th 2013). Starting from the solstice in June, the elevation angle decreased till the sun path intersected the PV array, causing a partial shading (September 14th 2013). Finally, during winter the sun path was almost completely covered by the PV array and only the diffuse light was received, determining a complete shading (December 14th 2013). On partial shading, the shadow usually cast on the OP during the central part of the day. Depending on the period of the year and the greenhouse zone, the shadow can affect most part of the day, thus with direct radiation only in the morning or in the evening. The pyranometers showed fluctuations due to the intermittent shadow cast by the metallic frame of the roof, which occasionally shaded the direct radiation. These fluctuations negatively affected the statistical parameters and are responsible for the light overestimation of the calculated values. However, the actual shadow cast by the greenhouse frame was not considered in the present algorithm, which purpose is to estimate the light distribution inside PV greenhouses only as a function of the PV array, independently from the greenhouse frames types. This assumption allows the application of the present algorithm to a broad variety of PV greenhouse types. These fluctuations were particularly accentuated when no shadow was on the OP (June 16th 2013), while they were mild or absent during partial or complete shading, since the diffuse radiation was less affected by the metallic frame.

According to the E-W orientation of the PV greenhouse, the shadow of the PV array moved from N to S in the first semester of the year, and from S to N in the second semester (Fig. 5). The E-W orientation enhances the global radiation incident in winter and decrease it in summer, when less irradiation is required by the crops (Sethi, 2009). During winter and most part of autumn, the sun elevation angle was low and the shadow cast mainly under the plastic cover, leaving the zones under the PV cover with direct radiation (Fig. 5a and d). As the sun elevation angle increased in springtime, the shadow gradually shifted under the PV array (Fig. 5b and c). This latter trend represents also the mean N-S distribution of the solar radiation during the year. In general, the less affected zones were the ones under the plastic cover, especially from April to September, where the G_{GR} was nearly 100%.

The yearly cumulated light distribution maps inside the PV greenhouse are shown in Fig. 6. The maps are presented at ground level (0.0 m) and at two canopy heights, for short crops (0.5 m) and tall crops (1.5 m). The N oriented span is occasionally affected by the shadow of the PV cover of the S oriented span. For this reason, the N span showed a G_{GR} averagely 6% lower than the S span during the year. This difference decreased as the canopy height increased and it was higher in winter (11% at 0.0 m) and not relevant in summer. The most shaded OPs under the PV cover received less than 31% G_{GR} on yearly basis, with the minimum value of 17% observed at 1.5 m. The mean G_{GR} under the PV cover ranged from 40% (at 2.0 m) to 57% (at 0.0 m), while it ranged from 59% (at 0.0 m) to 73% (at 2.0 m) under the plastic cover. Some zones close to the side walls and the gable walls were the least affected by shading, with a yearly G_{GR} values over 91%, especially at 1.5 m.

The yearly mean G_{GR} on the PV greenhouse area was 56%, ranging from 57 at ground level to 55% at 1.5 m (Table 2). The G_{GR} under the plastic cover reached up to 100% in summer, indicating limited or no shading at 1.5 and 2.0 m height. The yearly G_{GR} under the plastic cover increased with the canopy height by 14% from 0.0 to 2.0 m, while it decreased by 17% under the PV cover (G_{GR} from 57 at 0.0 m to 40% at 2.0 m). In fact, an opposite trend can be observed under the PV cover, where the highest values of G_{GR} were found during winter at ground level (up to 77% in January and February), which were consistently higher than the ones under the plastic cover. The G_{GR} under the PV cover usually decreased in summer.

The yearly CV on the greenhouse area was averagely 56% on all canopy heights, showing that the distribution of the global radiation on the greenhouse area was characterised by a high spatial variability. The CV on the transversal direction (N-S) was 55% on average, due to the path of the shadow cast by the PV array and it was 35% on the longitudinal direction (E-W). However, the CV on the longitudinal direction of the central portion of the PV greenhouse (set S1, S2 and S3) was only 3%, independently from the canopy height. This was due to the path of the shadow, which moved mainly in the N-S direction, while it moved also in the E-W direction on the zones close the gable walls (set G1 and G2), adding variability to the longitudinal distribution of the whole PV greenhouse area. These results indicate that inside an E-W oriented PV greenhouse, the global radiation is heterogeneously distributed only in the N-S direction, but it can be considered uniform in the longitudinal direction for most of the greenhouse area, except the zones close to the gable walls.

Table 1
Statistical validation of the model on the 10 pyranometers. All parameters are expressed as the mean of the 12 days of measurements with clear sky.

Pyranometer	Mean Daily Global Radiation (MJ m^{-2} d^{-1})	R^2	MBE (MJ m^{-2} d^{-1})	RMSE (MJ m^{-2} d^{-1})	RRMSE (%)
A	11.22	0.90	0.121	0.534	4.76%
B	3.30	0.94	0.068	0.374	11.35%
C	2.27	0.76	−0.021	0.331	14.56%
D	9.47	0.91	0.003	0.097	1.02%
E	2.65	0.80	0.044	0.219	8.27%
F	3.26	0.92	0.118	0.523	16.04%
G	2.67	0.89	0.016	0.453	16.94%
H	11.28	0.91	0.000	0.151	1.34%
I	1.90	0.84	0.036	0.207	10.89%
L	9.71	0.91	0.008	0.178	1.83%

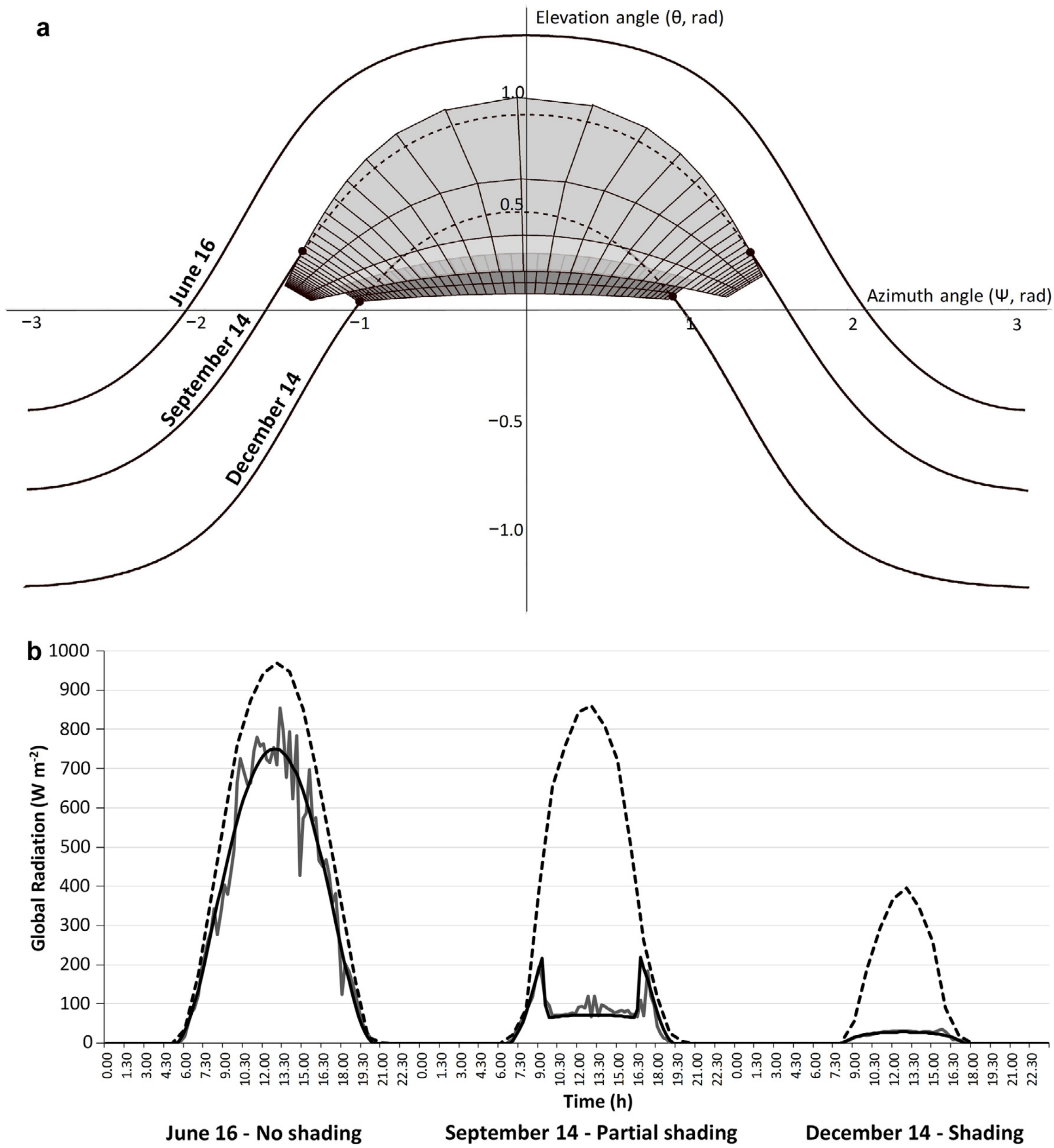

Fig. 4. Solar coordinates of the PV array and the sun path on the OP F at 1.3 m height (a), and related global radiation (b) during three exemplifying days with no shading (June 16, 2013 τ = 0.70, R^2 = 0.97), partial shading (September 14, 2013, τ = 0.60, R^2 = 0.84), and complete shading (December 14, 2013, τ = 0.49, R^2 = 0.97). All days were with clear sky conditions during measurements. In Fig. 4b: dashed curve is the measured I_G, grey line is the measured I_{GP} and black line is the calculated I_{GP}.

3.2. Implications of the cumulated light distribution on the agronomic sustainability of photovoltaic greenhouses

The light distribution maps highlighted the effects of the shading on the greenhouse area. The cumulated distribution data provided with the present model at yearly and monthly basis can be considered important inputs for the crop management inside PV greenhouses. The dynamic movement of the shadow on the PV greenhouse area suggested that the scenarios of light distribution change consistently, according to the period of the year and the height of the canopy. In particular, the global radiation increased with the canopy height under the plastic cover, and it decreases under the PV cover. Therefore, the growth stage of the crop and the related canopy height should be carefully considered when running crop models for the yield estimation inside PV greenhouses. Only the zones under the plastic cover and close to the side walls are compatible with the profitable cultivation of greenhouse crops, given the direct relation between illumination and photosynthetic rate (Challa, 1989). Ornamental species or nursery could be raised on the side walls, also using optimized upper stacks, to exploit the higher solar radiation at taller heights under the plastic cover. This possibility was already successfully tested on nursery plants inside a E-W oriented greenhouse, where upper and lower stacks were placed on the N oriented side wall, without affecting the crop yield at ground level (Sethi and Dubey, 2011).

The negative effects of the shading on crop yield was already described on tomato, indicating the importance of maximizing the light transmission of the greenhouse (Cockshull et al., 1992). The PV cover ratio under 20% has been tested on basil, tomato and cucumber, resulting in no yield losses but negative effects on quality parameters, such as the fruit size and color (Ureña-Sánchez et al., 2012; Minuto et al., 2009). Therefore, this latter

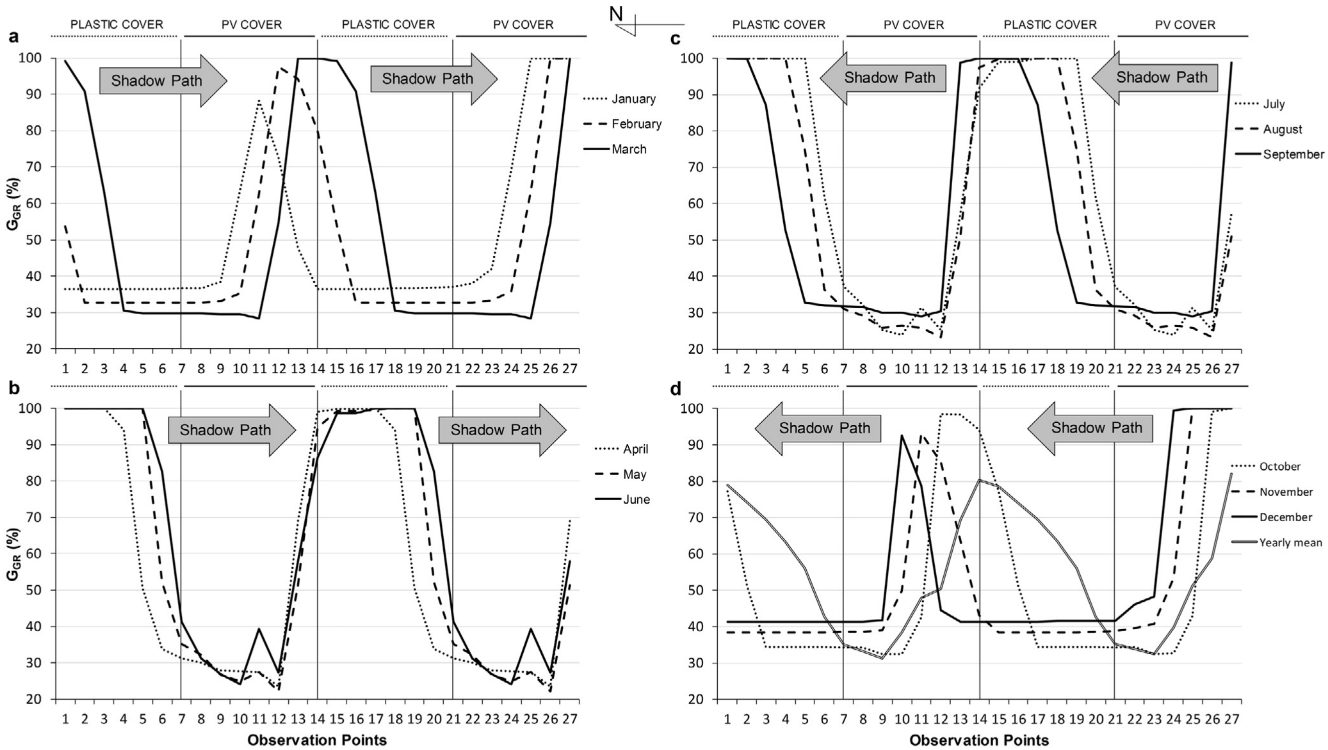

Fig. 5. Cumulated monthly distribution expressed as G_{GR} (%) on the greenhouse transversal direction (N-S) on 1.0 m height and estimated shadow path.

PV cover ratio should be considered the highest compatible with the most common greenhouse crops. Conversely, the cultivation of welsh onion suffered 25% yield loss inside a greenhouse with a PV cover ratio of 13% (Kadowaki et al., 2012). Furthermore, the insufficient solar radiation may cause a potential higher incidence of plant pathologies and require a specific crop protection approach. The cultivation cycle should start in a period with low shading, since heavy shading during juvenile stages may delay the development of the crop for the whole cycle (Marrou et al., 2013). As a consequence, for a PV greenhouse with 50% cover ratio, the cultivation should be conducted under the plastic cover and the cycle should start at the end of winter, to receive low or no shading during spring and summer. On the other hand, the shading of the PV modules contributes to decrease the temperature difference between the external and the internal environment. This effect, which has been extensively studied and applied to reduce the cooling load of the buildings (Dominguez et al., 2011), is useful during the hot periods to reduce the excessive heat load on the crops, without applying active cooling systems and contributing to keep the greenhouse temperature around the desired level. In the present PV greenhouse with 50% PV cover ratio, this difference was averagely 3 °C during the year and the PV panels released only 8% of the external global radiation inside the greenhouse as thermal energy (Cossu et al., 2014). This difference decreased with the increase of the shading level (Marucci and Cappuccini, 2016b).

Some strategies can be implemented to improve the environmental conditions for a crop inside a PV greenhouse. For example, the installation pattern of the PV panels on the roof affects the distribution of the solar radiation on the greenhouse area. Yano et al. showed that the checkerboard arrangement contributed to higher uniformity of light distribution in a gothic-arch roof greenhouse with 12.9% PV cover ratio, compared to the straight-line pattern (Yano et al., 2010; Fatnassi et al., 2015). The taller post height of the greenhouse and the homogenous distribution of the PV power on the roof area allows more solar radiation to enter from the gable and the side walls (Cossu et al., 2010). The orientation and the shape of a greenhouse should aim to maximize the total energy input on the greenhouse area: the orientation with one face to W and the other to E results in the highest amount of energy captured in winter (El-Maghlany et al., 2015). For elliptical shape greenhouses, the best results are achieved by using high aspect ratios (ratio between height and width) to maximize the solar radiation incident per square meter of cultivated land.

Specific PV technologies have been developed for the application on greenhouse roofs, improving the light transmissivity of the whole system, respect to conventional panels. The promising PV technologies already studied on PV greenhouse systems were the CIG and CIGS semiconductors, the flexible PV and thin films, the organic PV cells and the semi-transparent PV panels, also based on spherical micro-cells (Cossu et al., 2016; Emmott et al., 2015; Marucci et al., 2012; Minuto et al., 2011; Yano et al., 2014). Other solutions include the use of Fresnel lenses, which can be integrated in the south (S) oriented roof to concentrate the sunlight and produce both electrical and thermal energy (Sonneveld et al., 2011; Chemisana et al., 2012). The possibility to adjust the shading level caused by the PV panels has been studied in a prototype dynamic PV greenhouse for Mediterranean areas, where the PV panels can rotate along the longitudinal axis (Marucci and Cappuccini, 2016a). The PV panels acted as a passive cooling system able to protect the crops from high internal temperature in summer, conciliating the energy production with the light requirements of the crops (Marucci and Cappuccini, 2016b). Indeed, by adjusting the shading level, more light can reach the crop, compared to a PV greenhouse with fixed panels.

Many greenhouses with high PV shading have been already constructed in Europe and their agronomic sustainability is still under discussion and scientific investigation. However, the design modification of existing PV greenhouses to achieve a higher

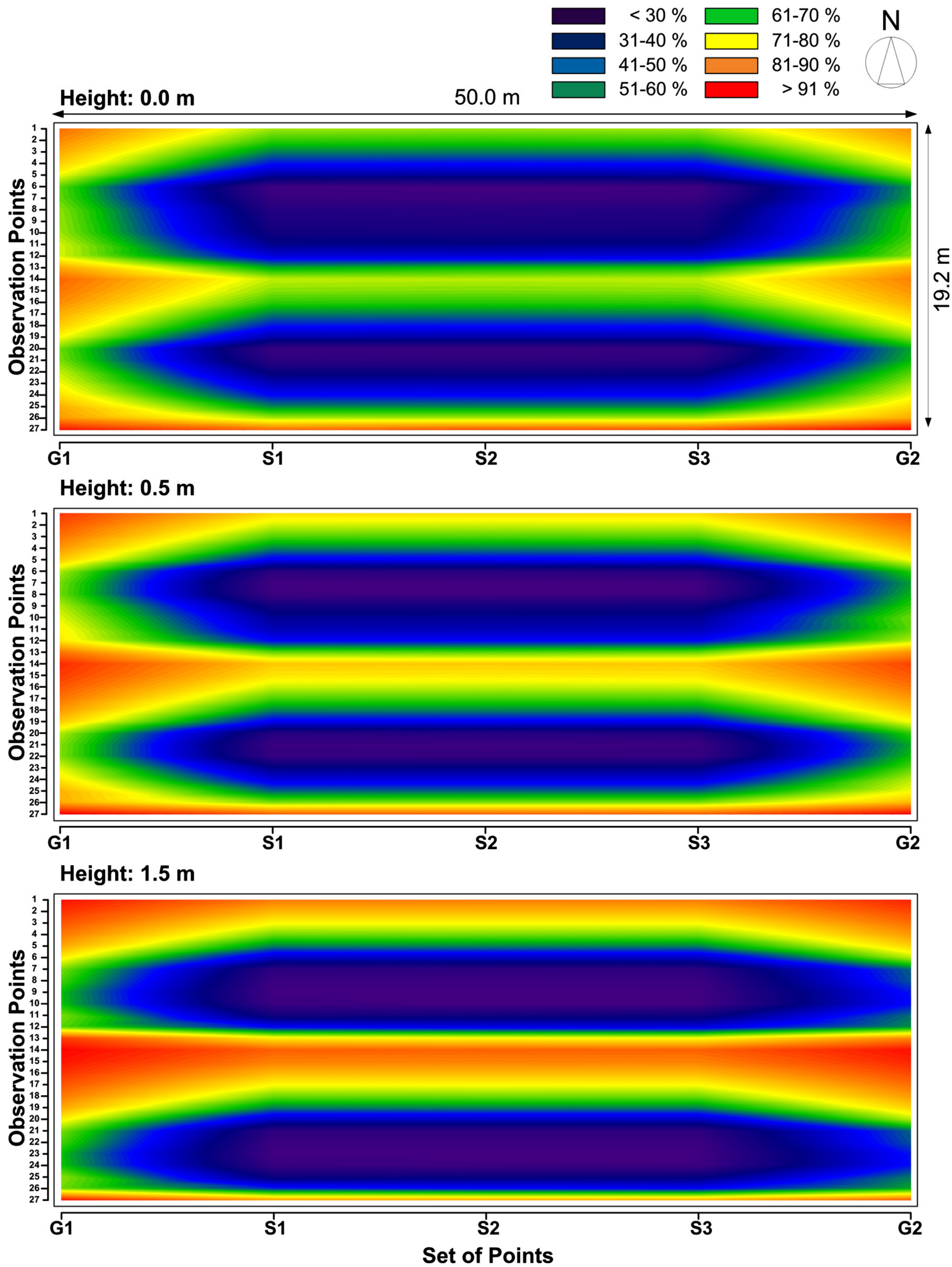

Fig. 6. Maps of the cumulated yearly light distribution on the PV greenhouse area, expressed as G_{GR} (%) on different canopy heights: ground level, 0.5 and 1.5 m.

irradiance is often not feasible under a technical and economic point of view, due to the high costs related to the partial reconstruction, including the modification of the PV panel installation patterns on the roof. For this reason, the strategies to improve the agronomic productivity of preexisting PV greenhouses should necessarily consider the crop management and the identification of suitable crops with low light requirements. The light distribution maps can be considered a valid decisional support tool to identify the best species and the portions of the greenhouse area suitable for a successful cultivation. With the present algorithm, these maps can be calculated for the most diffused PV greenhouse types. Subsequently, crop models can use the information concerning the light distribution to estimate the yield and development, focusing also on specific crop protection strategies.

Table 2
Monthly cumulated global radiation at different canopy heights under the plastic cover, the PV cover and on the whole greenhouse area. Data are expressed as G_{GR} (%). $p = 0.65$, $\tau = 0.60$.

Months	0.0 m			0.5 m			1.0 m			1.5 m			2.0 m		
	Plastic	PV	Greenhouse	Plastic	PV	Greenhouse	Plastic	PV	Greenhouse	Plastic	PV	Greenhouse	Plastic	PV	Greenhouse
January	38	77	56	37	74	53	37	66	50	36	58	46	41	44	44
February	33	77	53	33	70	50	36	60	48	44	48	47	55	32	45
March	43	61	52	50	55	53	57	45	51	65	38	52	72	28	50
April	71	45	58	75	40	57	80	34	57	84	29	56	88	34	60
May	88	36	61	90	31	60	92	31	61	95	35	63	98	45	70
June	92	31	61	93	32	62	97	34	65	100	41	69	100	54	75
July	90	33	61	92	31	61	93	33	62	97	38	66	100	49	73
August	78	40	58	82	36	58	85	30	57	89	30	59	92	38	63
September	55	57	56	61	49	55	67	42	55	73	33	53	80	30	55
October	35	74	54	38	66	52	44	57	51	53	44	49	61	30	46
November	40	79	58	39	75	55	38	67	51	40	57	48	46	42	45
December	45	75	61	42	74	57	41	69	54	41	59	49	41	48	45
Yearly mean	59	57	57	61	53	56	64	47	55	68	42	55	73	40	56

4. Conclusions

The agronomic sustainability of the PV greenhouse is strictly connected to the available incident global radiation and its distribution on the greenhouse area. The algorithm proposed in this paper is able to calculate the cumulated direct and diffuse radiation on the PV greenhouse area at the desired time interval and on different canopy heights. Geometric functions assimilating the PV panels to polygons are used to calculate the shading cast by the PV panels on designated points inside the greenhouse. To characterize the light distribution only as a function of the PV greenhouse type, the results have been expressed as the ratio of the cumulated global radiation inside the greenhouse with and without PV array on the roof. The simulations were conducted on a real E-W oriented greenhouse with a 50% PV cover ratio. Remarkable differences were observed on the ratio between the internal global radiation and the potential greenhouse global radiation without PV panels. These values ranged from 59 to 73% under the plastic cover and from 40 to 57% under the PV cover, depending on the canopy height considered (from 0.0 to 2.0 m). The differences were shown through maps of cumulated light distribution, which highlighted the greenhouse zones receiving the highest amount of solar radiation, thus the most suitable for cultivation. This algorithm can be used in perspective as a decisional support tool for choosing and managing crops inside PV greenhouses, based on their light requirements. Further studies will focus on the calculation of the light distribution maps for various existing PV greenhouse types. The structures will be compared and studied according to the light requirements of common and not conventional greenhouse crops, attempting to identify the most sustainable types and the best practices for crop management inside the PV greenhouses.

Acknowledgements

The authors thank the Regione Autonoma della Sardegna (Autonomous Region of Sardinia, Italy) for the financial support on the fundamental research project, LR 7/2007, "ORTILUX: Energy from photovoltaic greenhouse: study of the environmental parameters limiting the cultivation of tomato". We would like to thank also the Sardaflora-Cidam company and Mr. Murtas for his collaboration. This study was supported by JSPS (Japan Society for the Promotion of Science, Japan), with a post-doctoral fellowship (Grant No. 26·04085).

References

Al-Mahdouri, A., Gonome, H., Okajima, J., Maruyama, S., 2014. Theoretical and experimental study of solar thermal performance of different greenhouse cladding materials. Sol. Energy 107, 314–327. http://dx.doi.org/10.1016/j.solener.2014.05.006.

Attar, I., Farhat, A., 2015. Efficiency evaluation of a solar water heating system applied to the greenhouse microclimate. Sol. Energy 119, 212–224. http://dx.doi.org/10.1016/j.solener.2015.06.040.

Bambara, J., Athienitis, A., 2015. Experimental evaluation and energy modeling of a greenhouse concept with semi-transparent photovoltaics. Energy Proc. 78, 435–440. http://dx.doi.org/10.1016/j.egypro.2015.11.689.

Berlage, H.P., 1928. Zur Theorie der Beleuchtung einer horizontalen Fläche durch Tageslicht. Meteorol. Z. 45 (5), 174–180.

Bird, R.E., Hulstrom, R.L., 1980. Direct Insolation Models. Solar Energy Research Institute, Golden, CO. SERI/TR-335-344.

Blewett, T., Horne, M., Hill, R., 1997. Heliodon prediction of shading on building integrated photovoltaic systems. In: Proceedings of the 26th IEEE Photovoltaic Specialists Conference, Anaheim, CA, pp. 1393–1396.

Bojacá, C.R., Gil, R., Cooman, A., 2009. Use of geostatistical and crop growth modeling to assess the variability of greenhouse tomato yield caused by spatial temperature variations. Comput. Electron. Agric. 65, 219–227. http://dx.doi.org/10.1016/j.compag.2008.10.001.

Campiotti, C., Dondi, F., Genovese, A., Alonzo, G., Catanese, V., Incrocci, L., Bibbiani, C., 2008. Photovoltaic as sustainable energy for greenhouse and closed plant production system. Acta Hortic. (ISHS) 797, 373–378. http://dx.doi.org/10.17660/ActaHortic. 2008.797.53.

Capderou, M. (Ed.), 1985. Atlas solaire del'Algérie énergétique, Tome 2 vol. 2, OPU Algerno.: 2075-10-85; Alger, pp. 140–399.

Carlini, M., Honorati, T., Castellucci, S., 2012. Photovoltaic greenhouses: comparison of optical and thermal behaviour for energy savings. Math. Probl. Eng., 10 http://dx.doi.org/10.1155/2012/743764. Article ID 743764.

Carlini, M., Villarini, M., Esposto, S., Bernardi, M., 2010. Performance analysis of greenhouses with integrated photovoltaic modules. In: Taniar, D., Gervasi, O., Murgante, B., Pardede, E., Apduhan, B.O. (Eds.), Computational Science and Its Applications – ICCSA 2010, Lecture Notes in Computer Science, Part II, vol. 6017. Springer, Berlin, Heidelberg, pp. 206–214.

Castellano, S., 2014. Photovoltaic greenhouses: evaluation of shading effect and its influence on agricultural performances. J. Agric. Engine 45 (433), 168–174. http://dx.doi.org/10.4081/jae.2014.433.

Castellano, S., Santamaria, P., Serio, F., 2016. Solar radiation distribution inside a monospan greenhouse with the roof entirely covered by photovoltaic panels. J. Agric. Engine 47 (485), 1–6. http://dx.doi.org/10.4081/jae.2016.485.

Challa, H., 1989. Modeling for crop growth control. Acta Hortic. (ISHS) 248, 209–216.

Chemisana, D., Lamnatou, C., Tripanagnostopoulos, Y., 2012. The effect of Fresnel lens – solar absorber systems in greenhouses. Acta Hortic. (ISHS) 952, 425–432. http://dx.doi.org/10.17660/ActaHortic.2012.952.53.

Cockshull, K.E., Graves, C.J., Cave, C.R.J., 1992. The influence of shading on yield of glasshouse tomatoes. J. Hortic. Sci. 67, 11–24.

Collares-Pereira, M., Rabl, A., 1979. The average distribution of solar radiation-correlation between diffuse and hemispherical and daily and hourly insolation values. Sol. Energy 22, 155–164. http://dx.doi.org/10.1016/0038-092X(79)90100-2.

Cossu, M., Murgia, L., Caria, M., Pazzona, A., 2010. Economic feasibility study of semitransparent photovoltaic technology integrated on greenhouse covering structures. In: Proceedings of the International Conference Ragusa SHWA, Work Safety and Risk Prevention in Agro-food and Forest Systems. Ragusa Ibla Campus, Italy, pp. 648–655.

Cossu, M., Murgia, L., Ledda, L., Deligios, P.A., Sirigu, A., Chessa, F., Pazzona, A., 2014. Solar radiation distribution inside a greenhouse with south-oriented photovoltaic roofs and effects on crop productivity. Appl. Energy 133, 89–100. http://dx.doi.org/10.1016/j.apenergy.2014.07.070.

Cossu, M., Yano, A., Li, Z., Onoe, M., Nakamura, H., Matsumoto, T., Nakata, J., 2016. Advances on the semi-transparent modules based on micro solar cells: first integration in a greenhouse system. Appl. Energy 162, 1042–1051. http://dx.doi.org/10.1016/j.apenergy.2015.11.002.

Despotovic, M., Nedic, V., Despotovic, D., Cvetanovic, S., 2015. Review and statistical analysis of different global solar radiation sunshine models. Renew. Sust. Energy Rev. 52, 1869–1880. http://dx.doi.org/10.1016/j.rser.2015.08.035.

Dinesh, H., Pearce, J.M., 2016. The potential of agrivoltaic systems. Renew. Sust. Energy Rev. 15 (9), 4470–4482. http://dx.doi.org/10.1016/j.rser.2015.10.024.

Dominguez, A., Kleissi, J., Luvall, J.C., 2011. Effects of solar photovoltaic panels on roof heat transfer. Sol. Energy 85, 2244–2255. http://dx.doi.org/10.1016/j.solener.2011.06.010.

Dupraz, C., Marrou, H., Talbot, G., Dufour, L., Nogier, A., Ferard, Y., 2011. Combining solar photovoltaic panels and food crops for optimising land use: towards new agrivoltaic schemes. Renew. Energy 36 (10), 2725–2732. http://dx.doi.org/10.1016/j.renene.2011.03.005.

El Mghouchi, Y., El Bouardi, A., Choulli, Z., Ajzoul, T., 2016. Models for obtaining the daily direct, diffuse and global solar radiations. Renew. Sust. Energy Rev. 56, 87–99. http://dx.doi.org/10.1016/j.rser.2015.11.044.

El-Maghlany, W.M., Teamah, M.A., Tanaka, H., 2015. Optimum design and orientation of the greenhouses for maximum capture of solar energy in North Tropical Region. Energy Convers. Manage. 105, 1096–1104. http://dx.doi.org/10.1016/j.enconman.2015.08.066.

Emmott, C.J.M., Röhr, J.A., Campoy-Quiles, M., Kirchartz, T., Urbina, A., Ekins-Daukes, N.J., Nelson, J., 2015. Organic photovoltaic greenhouses: a unique application for semi-transparent PV? Energy Environ. Sci. 8, 1317–1328. http://dx.doi.org/10.1039/c4ee03132f.

Fatnassi, H., Poncet, C., Bazzano, M.M., Brun, R., Bertin, N., 2015. A numerical simulation of the photovoltaic greenhouse microclimate. Sol. Energy 120, 575–584. http://dx.doi.org/10.1016/j.solener.2015.07.019.

Gueymard, C., 2000. Prediction and performance assessment of mean hourly global radiation. Sol. Energy 68, 285–303. http://dx.doi.org/10.1016/S0038-092X(99)00070-5.

Kadowaki, M., Yano, A., Ishizu, F., Tanaka, T., Noda, S., 2012. Effects of greenhouse photovoltaic array shading on Welsh onion growth. Biosyst. Eng. 111, 290–297. http://dx.doi.org/10.1016/j.biosystemseng.2011.12.006.

Kitta, E., Baille, A.D., Katsoulas, N., Rigakis, N., Gonzàles-Real, M.M., 2014. Effects of the cover optical properties on screenhouse radiative environment and sweet pepper productivity. Biosyst. Eng. 122, 115–126. http://dx.doi.org/10.1016/j.biosystemseng.2014.04.001.

Kosugi, Y., Takanashi, S., Matsuo, N., Tanaka, K., Tanaka, H., 2006. Impact of leaf physiology on gas exchange in a Japanese evergreen broad-leaved forest. Agric. For. Meteorol. 139, 182–199. http://dx.doi.org/10.1016/j.agrformet.2006.06.009.

Li, M.F., Tang, X.P., Wu, W., Liu, H.B., 2013. General models for estimating daily global solar radiation for different solar radiation zones in main land China. Energy Convers. Manage. 70, 139–148. http://dx.doi.org/10.1016/j.enconman.2013.03.004.

Markvart, T., 2000. Solar Electricity. John Wiley & Sons, Chichester, UK.

Marrou, H., Guilioni, L., Dufour, L., Dupraz, C., Wery, J., 2013. Microclimate under agrivoltaic systems: is crop growth rate affected in the partial shade of solar panels? Agric. For. Meteorol. 177, 117–132. http://dx.doi.org/10.1016/j.agrformet.2013.04.012.

Marucci, A., Cappuccini, A., 2016a. Dynamic photovoltaic greenhouse: energy efficiency in clear sky conditions. Appl. Energy 170, 362–376. http://dx.doi.org/10.1016/j.apenergy.2016.02.138.

Marucci, A., Cappuccini, A., 2016b. Dynamic photovoltaic greenhouse: energy balance in completely clear sky condition during the hot period. Energy 102, 302–312. http://dx.doi.org/10.1016/j.energy.2016.02.053.

Marucci, A., Monarca, D., Cecchini, M., Colantoni, A., Manzo, A., Cappuccini, A., 2012. The semitransparent photovoltaic films for Mediterranean greenhouse: a new sustainable technology. Math. Probl. Eng., 14 http://dx.doi.org/10.1155/2012/451934. Article ID 451934.

Minuto, G., Tinivella, F., Bruzzone, C., Minuto, A., 2011. Con il fotovoltaico sul tetto la serra raddoppia la sua utilità. Supplemento a L'Informatore Agrario 2011 (38), 2–6.

Minuto, G., Bruzzone, C., Tinivella, F., Delfino, G., Minuto, A., 2009. Fotovoltaico sui tetti delle serre per produrre anche energia. Supplemento a L'Informatore Agrario 2009 (10), 16–21.

Page, J., 2003. The role of solar radiation climatology in the design of photovoltaic systems. In: Markvart, T., Castañer, L. (Eds.), Practical Handbook of Photovoltaics: Fundamentals and Applications. Elsevier, Oxford, UK, pp. 5–66.

Palva, L., Markkanen, T., Siivola, E., Garam, E., Linnavuo, M., Nevas, S., Manoochehri, F., Palmroth, S., Rajala, K., Ruotoistenmäki, H., Vuorivirta, T., Seppälä, I., Vesala, T., Hari, P., Sepponen, R., 2001. Tree scale distributed multipoint measuring system of photosynthetically active radiation. Agric. For. Meteorol. 106, 71–80. http://dx.doi.org/10.1016/S0168-1923(00)00171-4.

Perrin de Brichambaut, C., 1975. 'Estimation des Ressources Energétiques en France', Cahiersdel'A.F.E.D.E.S, N°1.

Pieters, J.G., Deltour, J.M., 1999. Modeling solar energy input in greenhouses. Sol. Energy 67, 119–130. http://dx.doi.org/10.1016/S0038-092X(00)00054-2.

Pollet, I.V., Pieters, J.G., 2002. PAR transmittances of dry and condensate covered glass and plastic greenhouse cladding. Agric. For. Meteorol. 110 (4), 285–298. http://dx.doi.org/10.1016/S0168-1923(01)00295-7.

Poncet, C., Muller, M.M., Brun, R., Fatnassi, H., 2012. Photovoltaic greenhouses, non-sense or a real opportunity for the greenhouse systems? Acta Hortic. (ISHS) 927, 75–79. 10.17660/ActaHortic.2012.927.7.

Quaschning, V., Hanitsch, R., 1998. Irradiance calculation on shaded surfaces. Sol. Energy 62 (5), 365–375. http://dx.doi.org/10.1016/S0038-092X%2898%2900018-8.

Reiter, R., Munzert, K., Sladkovic, R., 1982. Results of 5-year concurrent recordings of global, diffuse, and UV-radiation at three levels (700, 1800, and 3000 m a.s.l.) in the northern Alps. Theor. Appl. Climatol. Ser. B 30, 1–28.

Saïghi, M., 2002. Nouveau modèle de transfert hydrique dans le système sol- plante atmosphere (Thèse de Doctorat). USTHB, Alger.

Serrano-Arellano, J., Gijón-Rivera, M., Chávez-Servín, J.L., de la Torre-Carbot, K., Xamán, J., Álvarez, G., Belman-Flores, J.M., 2015. Numerical study of thermal environment of a greenhouse dedicated to amaranth seed cultivation. Sol. Energy 120, 536–548. http://dx.doi.org/10.1016/j.solener.2015.08.004.

Sethi, V.P., 2009. On the selection of shape and orientation of a greenhouse: thermal modeling and experimental validation. Sol. Energy 83, 21–38. http://dx.doi.org/10.1016/j.solener.2008.05.018.

Sethi, V.P., Dubey, R.K., 2011. Development of dual purpose greenhouse coupled with north wall utilization for higher economic gains. Sol. Energy 85, 734–745. http://dx.doi.org/10.1016/j.solener.2011.01.004.

Shen, C., He, Y., Liu, Y., Tao, W., 2008. Modelling and simulation of solar radiation data processing with Simulink. Simul. Model. Pract. Theor. 16, 721–735. http://dx.doi.org/10.1016/j.simpat.2008.04.013.

Sonneveld, P.J., Swinkels, G.L.A.M., van Tuijl, B.A.J., Janssen, H.J.J., Campen, J., Bot, G. P.A., 2011. Performance of a concentrated photovoltaic energy system with static linear Fresnel lenses. Sol. Energy 85, 432–442. http://dx.doi.org/10.1016/j.solener.2010.12.001.

Stone, R.J., 1993. Improved statistical procedure for the evaluation of solar radiation estimation models. Sol. Energy 51 (4), 289–291. http://dx.doi.org/10.1016/0038-092X(93)90124-7.

Supit, I., Van Kappel, R.R., 1998. A simple method to estimate global radiation. Sol. Energy 63, 147–160. http://dx.doi.org/10.1016/S0038-092X(98)00068-1.

Tanaka, K., Kosugi, Y., Nakamura, A., 2002. Impact of leaf physiological characteristics on seasonal variation in CO_2, latent and sensible heat exchanges over a tree plantation. Agric. For. Meteorol. 114, 103–122. http://dx.doi.org/10.1016/S0168-1923(02)00128-4.

Ureña-Sánchez, R., Callejón-Ferre, Á.J., Pérez-Alonso, J., Carreño-Ortega, Á., 2012. Greenhouse tomato production with electricity generation by roof-mounted flexible solar panels. Sci. Agric. 69 (4), 233–239. http://dx.doi.org/10.1590/S0103-90162012000400001.

Wan Nik, W.B., Ibrahim, M.Z., Samo, K.B., Muzathik, A.M., 2012. Monthly mean hourly global radiation estimation. Sol. Energy 86, 379–387. http://dx.doi.org/10.1016/j.solener.2011.10.008.

Wolfram Research Inc, 2014. Mathematica, Version 10.0, Champaign, IL.

Woyte, A., Nijs, J., Belmans, R., 2003. Partial shadowing of photovoltaic arrays with different system configurations: literature review and field test results. Sol. Energy 74, 217–233. http://dx.doi.org/10.1016/S0038-092X%2803%2900155-5.

Yano, A., Furue, A., Kadowaki, M., Tanaka, T., Hiraki, E., Miyamoto, M., Ishizu, F., Noda, S., 2009. Electrical energy generated by photovoltaic modules mounted inside the roof of a north-south oriented greenhouse. Biosyst. Eng. 103 (2), 228–238. http://dx.doi.org/10.1016/j.biosystemseng.2009.02.020.

Yano, A., Kadowaki, M., Furue, A., Tamaki, N., Tanaka, T., Hiraki, E., Kato, Y., Ishizu, F., Noda, S., 2010. Shading and electrical features of a photovoltaic array mounted inside the roof of an east-west oriented greenhouse. Biosyst. Eng. 106, 367–377. http://dx.doi.org/10.1016/j.biosystemseng.2010.04.007.

Yano, A., Onoe, M., Nakata, J., 2014. Prototype semi-transparent photovoltaic modules for greenhouse roof applications. Biosyst. Eng. 122, 62–73. http://dx.doi.org/10.1016/j.biosystemseng.2014.04.003.

Yoo, S.H., 2011. Simulation for an optimal application of BIPV through parameter variation. Sol. Energy 85, 1291–1301. http://dx.doi.org/10.1016/j.solener.2011.03.004.

Yoo, S.H., 2015. Energy Science and Technology Series. Solar Engineering-I, "Ecological Criteria for Optimization of Solar Architecture", vol. 5. Studium Press LLC, Houston, USA. ISBN:1-62699-066-2.